Analysis of Tribo-Electric Charging of Spherical Beads Using Distinct Element Method

Tatsushi Matsuyama[1], Enes Šupuk[2], Hossein Ahmadian[2], Ali Hassanpour[2] and Mojtaba Ghadiri[2]

[1] *Faculty of Engineering, Soka University, Tokyo 192-8577, Japan*
[2] *Institute of Particle Science and Engineering, University of Leeds, Leeds, LS2 9JT, UK*

Abstract Tribo-electrification is an important phenomenon in powder handling, as it could cause hazards and nuisance, such as dust explosion, adhesion to walls and blockage of pipelines leading to powder losses and difficulties in flow control. At present, there are only a few methods available to predict the dynamic charging of bulk powders, and they are not suitable for testing a small quantity of powders or handling highly active powders, for which full isolation would be needed. In this paper, the operation of a simple test device is analysed. Tribo-electrification of a single spherical bead inside a sealed capsule is induced through a horizontal motion using a shaking device at various frequencies. The single particle contact charge obtained from experiments is incorporated in numerical simulations based on Distinct Element Method (DEM) and is used to predict the transient charge accumulation of an assemblage of beads. In the model, the tribo-charging of a single bead is related to the contact area of the bead on impact with the capsule wall. The effects of long range forces, space charge and image charge at boundary condition are investigated for bulk charging. It is shown that the inclusion of space charge effects and boundary condition into the DEM model leads to a better prediction of charge build-up when compared with the experimental results.

Keywords: Electrostatic; Tribo-Electric; Distinct Element Method; DEM; Simulation.
PACS: 41.20.Cv

INTRODUCTION

Powder handling operations cause particles to frequently make contacts with each other and with a variety of boundary surfaces. Such contacts result in particles acquiring electrostatic charges due to the process of tribo-charging. These electrostatic charges can cause powder deposition [1] resulting in the loss of powder [2] and segregation [3] which ultimately affects the product quality. The ability to control the charging of powders is therefore essential in powder handling. For this purpose a simple test device [4] has been developed to characterise the tribo-electric charging propensity of powders. The test device consists of a shaking machine and a set of shaking capsules. The charge on particles is quantified using a Faraday cup and an electrometer before and after shaking. The sample of beads is placed inside a capsule and shaken by reciprocal strokes in a horizontal direction. It is desirable to assess the tribo-electrification of an assemblage of particles, as it is more relevant to actual industrial processes involving bulk powders. However, it is difficult to analyse the particle charging characteristics inside the shaking capsule due to multiple particle-wall and particle-particle contacts in addition to space charge effects on charge exchange processes. In this paper, firstly the tribo-electrification of a single spherical bead inside a sealed capsule is analysed experimentally and by DEM simulations. An empirical model, based on a first-order charging rate, is then fitted to the data relating the accumulated charge to the contact area of the bead with the capsule walls due to impact and/or sliding contacts. This is then used in the DEM simulations of assemblages of beads and a comparison is made with experiments at different shaking frequencies. Furthermore, the effects of long range forces, space charge and image charge at boundary conditions are investigated.

EXPERIMENTAL

Porous alumina beads, used in the oil industry as catalyst carriers for hydrocracking, were used in the experimental work due to their large size (2 mm) as this eliminated the possibility of particles adhering to capsule walls minimising charge loss through adhered particles. The alumina beads were produced by a sol-gel process, and hence were highly spherical in shape (with an aspect ratio of 1.05) with smooth surfaces, making them ideal for DEM simulations. Furthermore, these beads have a large crushing strength [5] and are unlikely to break during shaking at high frequencies. As a result complications due to the presence of additional charged debris will be avoided. A Retsch shaking machine with a Faraday cup and an electrometer was used. A full description of the device and exact procedure is given by Šupuk *et al.* [4]. Depending on the experiment, either a single bead or a small mass of beads (typically around 1 g) was placed inside a 10 ml capsule. The capsule was then subjected to reciprocal vibrations in a horizontal direction. Depending on the vibration frequency, the beads impacted alternately against the rounded ends of the capsule. The capsule used in these experiments was made out of Polytetrafluoroethylene (PTFE). The vibration frequency could be set precisely between 3 and 30 Hz. To measure the electrostatic charge on beads, a Faraday cup connected to an electrometer (Keithley Model 6514) was used.

Single Bead Experiments

A single alumina bead, 2 mm in diameter, was tribo-charged at 10, 20 and 30 Hz frequencies inside a shaking capsule. The average mass of a single alumina bead is 4.4 ± 0.1 mg based on a random selection of 30 beads. Initially, each alumina bead was treated with ethanol and dried in oven at 35 °C for one hour prior to tribo-charging tests. Following charge measurement, the alumina bead was discarded. The inner surfaces of the PTFE capsule was wiped with ethanol and dried. The following test was carried out with a fresh bead. This procedure was repeated a minimum of three times for each tribo-charging test and the average value was used. It should be noted that there was no breakage of alumina particles during the single particle tests at all three frequencies. The temperature and humidity range during single particle testing was 20.1-24.1 °C and 34.1-42.3 % RH, respectively.

The experimental results for single alumina beads tribo-charged at three test frequencies are shown in Fig. 1. The charge values for 20 and 30 Hz shaking frequencies are close to each other, whilst those at 10 Hz are distinctly different. At 10 Hz, the time taken to reach the saturation charge is longer. This is most likely due to a smaller number of shaking cycles, as compared to those of the other two frequencies, and consequently a lower number of particle-wall contacts as well as lower impact velocities. A first order charging rate equation (Eq. 1) proposed by Hogue *et al.* [6] was fitted to the experimental data by linear regression.

$$q = q_{sat}(1 - e^{-\alpha t}) \qquad (1)$$

where q_{sat} is the saturated charge and t is time. The fitted values are summarised in Table 1. The results show the charging rate constant is much higher at frequencies of 20 and 30 Hz as compared to that obtained at 10 Hz.

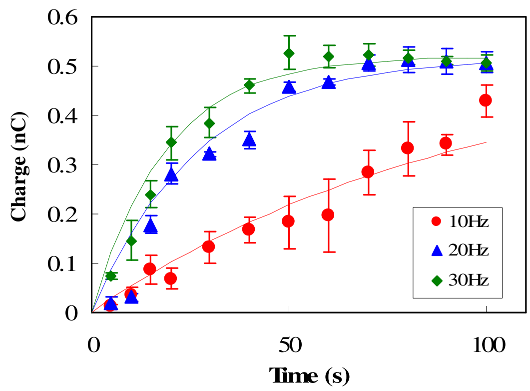

FIGURE 1. Charge on single alumina beads as a function of shaking time following tribo-charging at 10, 20 and 30 Hz frequencies – lines show best fit using Eq. 1.

TABLE 1. α values for single and bulk tests of alumina beads.

Frequency	SINGLE		BULK	
[Hz]	α [s^{-1}]	q_{sat} [nC]	α [s^{-1}]	q_{sat} [nC]
10	0.0109		0.0036	31.34
20	0.0371	0.52	0.0144	32.18
30	0.0539		0.0136	30.95

Bulk Shaking Experiments

Two hundred and thirty alumina beads, corresponding to 1.012 ± 0.001 g, were used for bulk tribo-charging tests. These tests were carried using the exact procedure described for the single beads with a PTFE shaking capsule at time intervals 1, 3, 5 and 10 minutes. A minimum of three runs were performed for each test. The charge on the beads was measured for each run and then averaged. The beads were then weighed to determine any mass loss due to breakage.

The temperature and humidity ranges during bulk particle testing were 20.7-23.3 °C and 35.8-47.4 % RH, respectively. The experimental results obtained at three test frequencies are presented in Fig. 2. Initially, the level of charge measured at 10 Hz was considerably lower than those at 20 and 30 Hz. However, as the length of shaking time is increased, the charge on the beads at the three test frequencies approach asymptotically a saturated charge level. The saturated charge q_{sat} levels at each frequency are also shown in Table 1. As with the single beads results, a first order charging rate equation (Eq. 1) was fitted to the bulk shaking data by linear regression. The values of the rate constant α are summarised in Table 1. The results show the charging rate constant is lowest at 10 Hz. Interestingly, the value of the charging rate constant is highest at 20 Hz (not 30 Hz) for bulk shaking. This may suggest that at 20 Hz the beads-wall contact frequency as well as the impact velocity is the highest. This is investigated further using DEM in the next section. Furthermore, it may be noted that the charge on the bulk beads is not 230 times higher than on a single bead. This may suggest that when the beads are shaken in bulk, the probability of individual beads making contact with the capsule walls decreases. There are also other hindering effects due to long range forces, space charge and image charge at boundaries.

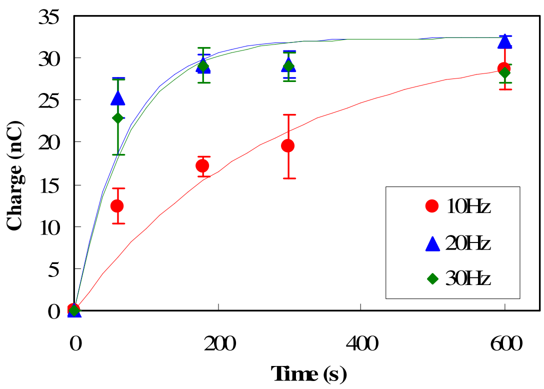

FIGURE 2. Charge of 230 alumina beads following tribo-charging at 10, 20 and 30 Hz frequencies – lines show best fit using Eq. 1.

SIMULATION RESULTS

Calibration Procedure

The simulations were performed using the Distinct Element Method, a methodology that was originally proposed by Cundall and Strack [7] and implemented in PFC^{3D} software (ITASCA). The DEM models the interaction between contiguous particles as a dynamic process and the time evolution of the particles is advanced using an explicit finite difference scheme. The interactions between the constituent particles are based on theories of contact mechanics. In this work a linear contact model is used to simulate particle-particle and particle-wall interactions. The mechanical properties of the alumina beads were measured by Couroyer *et al.* [5] and are shown in Table 2. The ends of the capsule are designed by arranging five cone frustums around a cylinder positioned in the central region as shown in Fig. 3. The stiffness of the PTFE walls is lower than the alumina beads and was estimated using the elastic modulus.

Table 2. Alumina beads and PTFE wall properties.

Property	Value
Particle Diameter	2 mm
Particle Friction	0.5
Particle Normal Stiffness	0.3 MN/m
Particle Tangential Stiffness	0.25 MN/m
Particle density	1100 kg/m^3
Contact Damping factor	0.12
Wall normal stiffness	0.1 MN/m
Wall tangential stiffness	0.082 MN/m
Wall friction	0.5

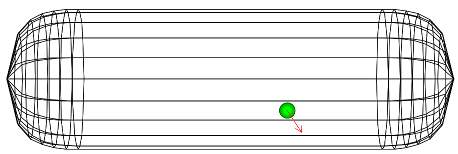

FIGURE 3. A single bead inside the shaking capsule.

Initially, a single sphere representing an alumina bead was simulated inside the capsule. The capsule was then vibrated at frequencies of 10, 20 and 30 Hz at an amplitude identical to the experimental device (simple harmonic motion). The maximum contact area for every particle-wall contact event was then recorded, as it is the main factor affecting the charge transfer [8]. For a single contact event, the charge transfer was calculated by the linear relationship (Eq. 2) between the charge transfer Δq and the charge, q, held by the particle just before the contact:

$$\Delta q = \beta \Delta S \left(1 - \frac{q}{q_{sat}} \right), \qquad (2)$$

where β is the proportionality constant and ΔS is the maximum contact area. An integration of Eq. 2 from $q=0$ yields,

$$q = q_{sat} \left(1 - e^{-\beta \sum \Delta S / q_{sat}} \right). \qquad (3)$$

For a longer time scale, the accumulated maximum contact area can be treated as proportional to the operation time,

$$\sum \Delta S = \gamma t \qquad (4)$$

therefore, Eq. 3 can be converted into Eq. 5:

$$q = q_{sat} (1 - e^{-\gamma \beta t / q_{sat}}) \qquad (5)$$

This converts the time constant α in Eq.1 to the accumulated contact area as a function of time, expressing a more practical term of physical event, and provides a basis to analyse the macroscopic charge development on single particles with the aid of DEM simulations. In the calculation, constants β and q_{sat}

were fitted parameters obtained from the experimental data.

Bulk Simulations

With the calibrated parameters, the simulation procedure was applied to bulk shaking with 230 particles. For a first attempt, the single particle procedure was simply applied without any extensions of electrostatic functions, which will be described in detail later. The results were simply given as 230 times of the single particle cases. However the trends given by these values did not correspond exactly to the experimental results obtained (Fig. 4, dashed lines).

In the next stage, a number of necessary electrostatic functions were incorporated into the DEM simulations for bulk shaking,. These were long range forces, space charge effects, and boundary conditions.

For the boundary conditions, equipotential or conductive conditions on the capsule surfaces were considered. However, this differed from the actual experiments, where the capsule was made of PTFE, a non-conductive polymer, and hence this assumption could have affected the calculation results. This point should be addressed in future investigations. There are a range of options to calculate the electric field distribution inside the capsule. In this work a charge simulation method was employed with discrete image charge array located outside the capsule.

The electrostatic field was calculated by the superimposition principle, whereby the contributions from every particle charge was added, including the virtual charges. The resulting electrostatic field affects an object not only by way of the external force (the long range force) but also in the charge exchange (space charge effect). In the simulation procedure, the long range force was calculated by Coulomb's law. For the space charge effect, an electric field equivalent method was used in which the charge q in Eq. 2 was modified with an additional charge giving an equivalent field to the external field (space charge effect) at the particle surface.

The results following the incorporation of all the electrostatic functions are shown in Fig. 4 (solid lines), where a drastic improvement is observed. The level of saturated charge has been significantly reduced; however it is still overestimated. There are several factors that could affect the level of saturated charge, such as the boundary conditions. In the simulations the walls are conductive and do not represent the actual experimental conditions. Additionally, the field equivalent method used to calculate space charge effect may be too simplistic. Such factors should be studied in detail in the future. It should also be noted that the long range force resulted in the expansion of the particle bed to some extent; however, the effect of the shaking frequency was more notable and the role of the bed expansion is not clear at this moment.

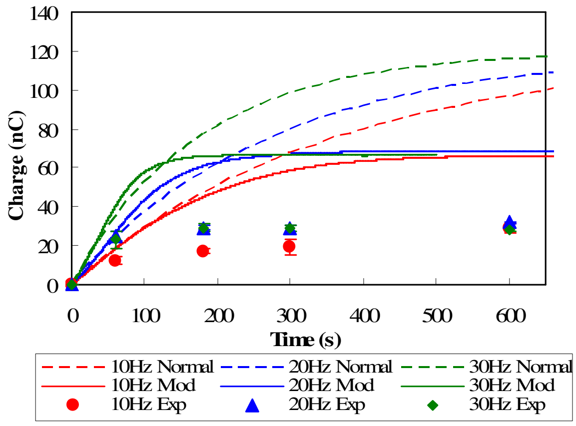

FIGURE 4. Comparison of experimental charge accumulation on 230 alumina beads at three test frequencies with simulations predictions with and without long range force, space charge and image charge at the boundaries.

CONCLUSIONS

Tribo-electrification of spherical beads inside a horizontally shaken sealed capsule has been analysed experimentally and simulated using a DEM model. An empirical first order rate equation, based on experimental data, has been incorporated in the DEM simulations. It is found that the model significantly overestimates the total charge build-up for bulk shaking, as compared with the experimental results. However, the inclusion of space charge effects and boundary condition into the DEM model significantly improves the prediction of total charge build up.

REFERENCES

1. X. J. Zheng, N. Huang, and Y. H. Zhou, *Eur. Phys. J.* **19,** 129-138 (2006)
2. C. U. Yurteri, M. K. Mazumder, N. Grable, G. Ahuja, S. Trigwell, A. S. Biris, R. Sharma and R. A. Sims, *Part. Sci. Technol.,* **20,** 59-79 (2002)
3. D. K. Yanar, and B. A. Kwetkus, *J. Electrostat.,* **35,** 257-266 (1995)
4. E. Šupuk, C. Seiler and M. Ghadiri, *Part. Part. Syst. Charact.,* Submitted (2008)
5. C. Couroyer, Z. Ning and M. Ghadiri, *Powder Technol.,* **109,** 241-254 (2000)
6. M.D. Hogue, C.I. Calle, P.S. Weitzman and D.R. Curry, *J. Electrostat.*, **66**, 32-38, 2008.
7. P. A. Cundall and O. D. L Strack, *Geotechnique*. **29**, 47-65 (1979).
8. S. Matsusaka, M. Ghadiri and H. Masuda, *J. Phys. D: Appl. Phys.,* **33,** 2311-2319 (2000).